ACS Combinatorial Science

Research Article

pubs.acs.org/acscombsci

Design of High-Throughput Screening Assays and Identification of a SUMO1-Specific Small Molecule Chemotype Targeting the SUMO-Interacting Motif-Binding Surface

Aileen Y. Alontaga,[†] Yifei Li,[†] Chih-Hong Chen,[†] Chen-Ting Ma,[‡] Siobhan Malany,[§] Danielle E. Key,[§] Eduard Sergienko,[‡] Qing Sun,[‡] David A. Whipple,[∥] Daljit S. Matharu,[∥] Baozong Li,[†] Ramir Vega,[†] Yi-Jia Li,[†] Frank J. Schoenen,[∥] Brian S. J. Blagg,[∥] Thomas D.Y. Chung,[‡] and Yuan Chen*,[†]

[†]Department of Molecular Medicine, Beckman Research Institute of the City of Hope, Duarte, California 91010, United States

[‡]Conrad Prebys Center for Chemical Genomics, Sanford-Burnham Institute, La Jolla, California 92037, United States

[§]Conrad Prebys Center for Chemical Genomics, Sanford-Burnham Institute at Lake Nona, Orlando, Florida 32827, United States

[∥]University of Kansas Specialized Chemistry Center, Lawrence, Kansas 66049, United States

Supporting Information

ABSTRACT: Protein−protein interactions are generally challenging to target by small molecules. To address the challenge, we have used a multidisciplinary approach to identify small-molecule disruptors of protein−protein interactions that are mediated by SUMO (small ubiquitin-like modifier) proteins. SUMO modifications have emerged as a target with importance in treating cancer, neurodegenerative disorders, and viral infections. It has been shown that inhibiting SUMO-mediated protein−protein interactions can sensitize cancer cells to chemotherapy and radiation. We have developed highly sensitive assays using time-resolved fluorescence resonance energy transfer (TR-FRET) and fluorescence polarization (FP) that were used for high-throughput screening (HTS) to identify inhibitors for SUMO-dependent protein−protein interactions. Using these assays, we have identified a nonpeptidomimetic small molecule chemotype that binds to SUMO1 but not SUMO2 or 3. NMR chemical shift perturbation studies have shown that the compounds of this chemotype bind to the SUMO1 surface required for protein−protein interaction, despite the high sequence similarity of SUMO1 and SUMO2 and 3 at this surface.

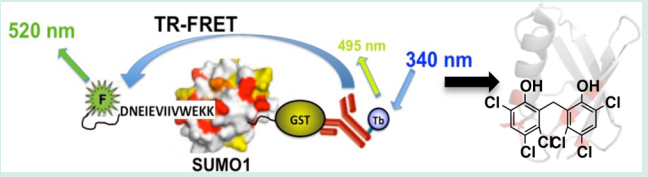

KEYWORDS: *small ubiquitin-like modifier (SUMO), TR-FRET, fluorescence polarization, SUMO-interacting motif (SIM)*

INTRODUCTION

Despite the important roles of protein−protein interactions (PPI) in cellular regulation, it has been difficult to modulate these interactions with small molecules. With increased studies in this area, we can begin to identify and develop effective approaches to discover small molecule PPI modulators. In this study, we used a multidisciplinary approach including both biochemical and biophysical methods to address PPI mediated by small ubiquitin-like modifiers (SUMO).

SUMO proteins are ubiquitin homologues that can conjugate to other cellular proteins through a biochemical mechanism similar to ubiquitination. Emerging data indicate that SUMOylation is a potential target for developing therapies for cancer and other life-threatening diseases. SUMOylation is important for major oncogenesis pathways, such as those driven by c-Myc,[1] and thus could be targeted for anticancer therapy when these oncogenes are activated. In addition, SUMOylation regulates the DNA-damage response that is important to cancer therapy, allowing it to be targeted to either enhance cancer cell sensitivity to DNA-damaging chemo and radiation therapy, or to inhibit the aberrant DNA repair pathways to induce cell death.[2] Besides cancer, SUMOylation is involved in the development of neurodegenerative disorders, such as Huntington's disease[3] and pathogen infection.[4] SUMO conjugation does not lead to protein degradation directly, but enables protein−protein interactions through SUMO-interacting motifs (SIM).[5]

At least three SUMO paralogs, SUMO1, 2, and 3, are expressed in human cells and conjugate to other proteins.[6] SUMO1 shares less than 50% sequence identity to other SUMO isoforms. However, SUMO2 and 3 are nearly identical in sequence and cannot be distinguished by antibodies. In particular, the surfaces of SUMO2 or 3 that bind SIM have identical amino acid residues. However, the various SUMO paralogs appear to have distinct functions. For example, SUMO2 and SUMO3 conjugations respond strongly to environmental stress, such as heat shock, while SUMO1 conjugation does not.[7] In addition, the cellular localization patterns of the SUMO paralogs do not completely overlap. SUMO-1 primarily localizes to the nuclear pore and nucleolus,

Received: December 1, 2014
Revised: February 25, 2015
Published: February 26, 2015

DOI: 10.1021/co500181b
ACS Comb. Sci. 2015, 17, 239−246

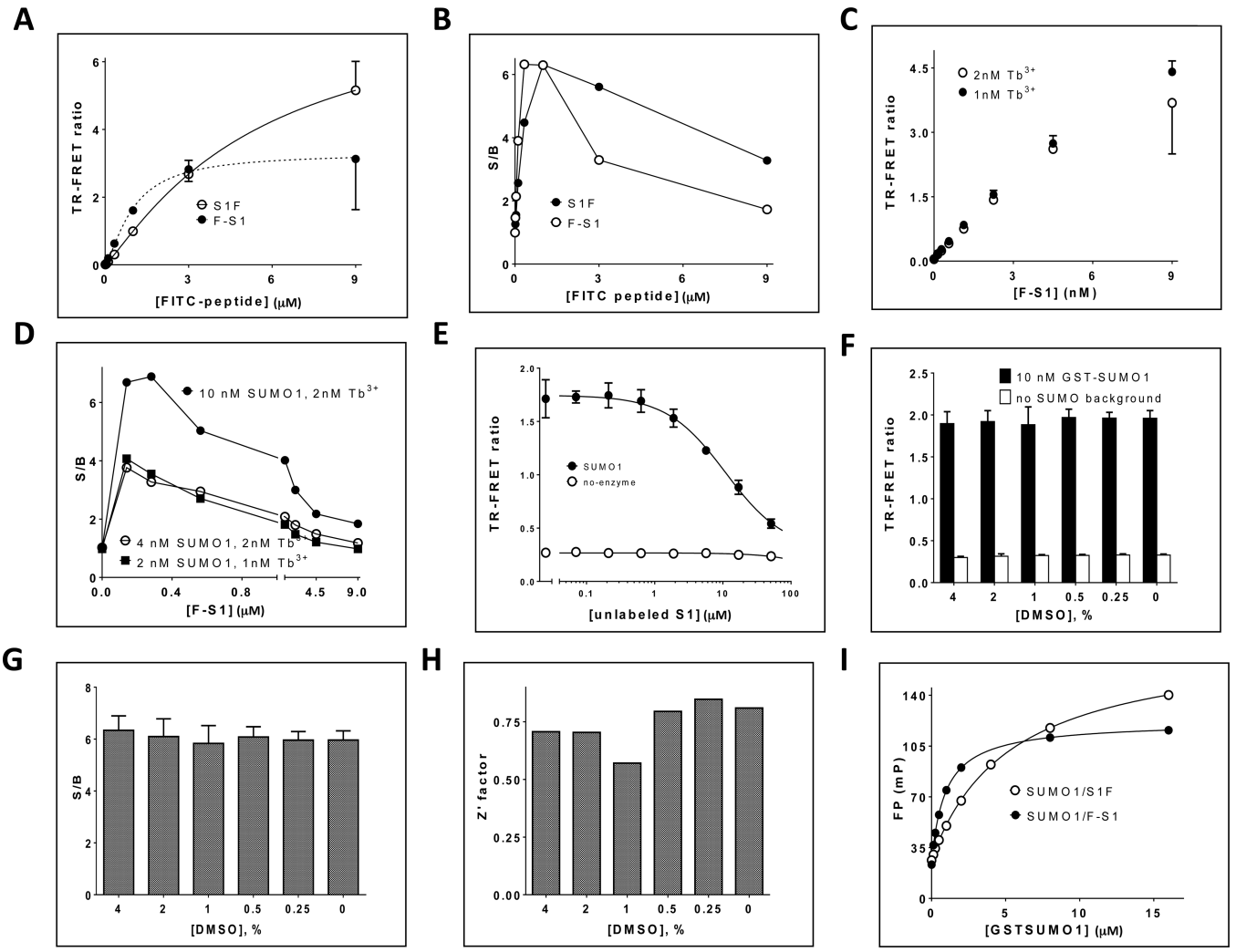

Figure 1. FRET assay development for SUMO1−S1. (A) Titration of N-terminal fluorescein-tagged (F-S1) or C-terminal fluorescein-tagged (S1F) S1 peptide with 2 nM Tb-anti-GST and 10 nM GST-SUMO1. Signal was background-subtracted. EC_{50} were determined to be 1.0 ± 0.067 and 5.5 ± 0.038 μM for F-S1 and S1F, respectively. Assay windows were 33000 ± 1100 units (FRET Ratio 520 nm/490 nm × 10000, unless otherwise noted) and 81000 ± 360 units, respectively. (B) Corresponding signal/background (S/B) plot for panel A. (C) Background fluorescence without SUMO1. Linear increase of background decreases S/B. (D) Donor optimization. Two nanomolar Tb-anti-GST and 10 nM GST-SUMO1 were confirmed to be the optimal condition. (E) Displacement dosage response curve. Unlabeled S1 competed effectively with F-S1 for GSTSUMO1 binding. IC_{50} was determined to be 11 ± 0.6 μM. (F) DMSO effect (32 wells per each condition). No signal change for 0.5% DMSO or lower. (G and H) Corresponding S/B plot and Z' factor at various DMSO concentrations. (I) FP Assay development for SUMO1-S1. Titration of GST-SUMO1 against 7 nM N-terminal tagged (F-S1) or C-terminal tagged (S1F) S1. Assay window were 99 ± 1.2 and 150± 5.0 mP, respectively. EC_{50} were 940 ± 27 and 5400 ± 350 nM, respectively.

but SUMO2 and 3 primarily localize in the nucleoplasm and nuclear bodies.[8] Furthermore, SUMO1 and SUMO2 conjugation to the same protein could have opposing functions.[9] Small-molecule modulators of SUMO-SIM interactions with paralog-specificity would be very helpful for elucidating the functions of the different SUMO paralogs. Because the SIM sequence is short, it was not surprising that we previously found peptidomimetics that have low affinity to bind all SUMO proteins (K_d ≈ 1 mM). Conjugation of these molecules to nanoparticles achieved high affinity for binding poly-SUMO chains due to the multivalency effect.[10] Recently, nonpeptidomimetic small molecule modulators of SUMO-SIM interaction were described, but these molecules bind all SUMO paralogs without specificity.[11] Small-molecule modulators that bind to a SUMO protein with paralog-specificity have not been reported.

In this study, we developed biochemical HTS assays that were used to detect SUMO1 interaction with a SUMO1-specific-SIM peptide using time-resolved fluorescence resonance energy transfer (TR-FRET) and fluorescence polarization (FP) assay formats. Using these assays, we screened a ∼365 000 compound library and identified a SUMO1-specific nonpeptidomimetic compound that targets the SIM-binding surface. Analogs of the initial hits have revealed the conformational flexibility of the compounds as important for binding affinity to SUMO1. This study not only provides the method for identification of SUMO paralog-specific SUMO-SIM interaction inhibitors, but also demonstrates that it is feasible to identify such small molecules, which are not peptidomimetics, despite the high sequence identity of the SIM-binding surfaces of the different SUMO paralogs.

DOI: 10.1021/co500181b
ACS Comb. Sci. 2015, 17, 239−246

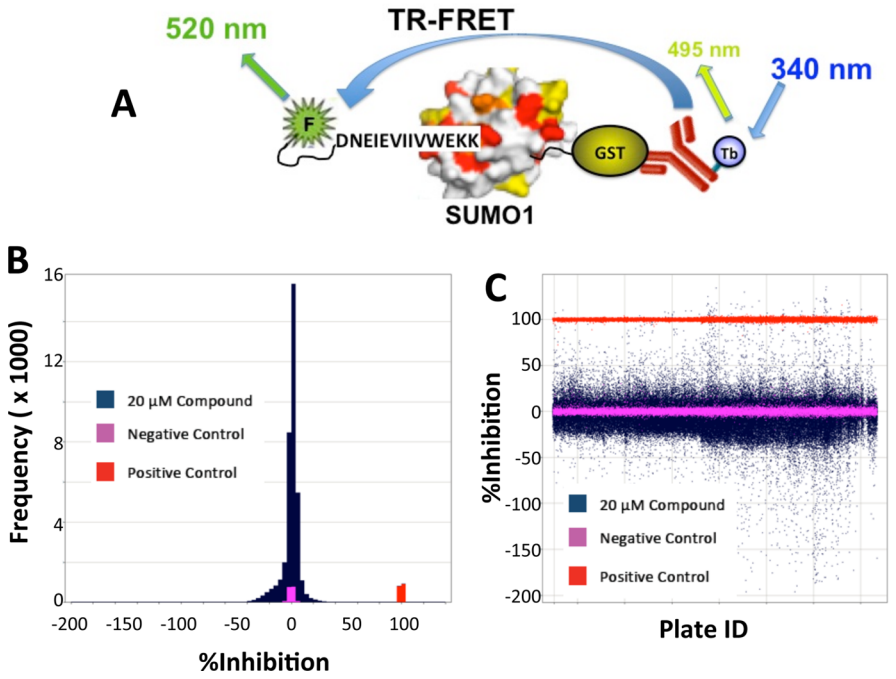

Figure 2. Primary high-throughput screen of a large library (~365 000 compounds) with a SUMO1-S1 TR-FRET assay. (A) Schematic of primary assay. (B) Frequency distribution of inhibitory activity of the chemical library. (C) Scatterplot of individual inhibitory activity by plate ID.

RESULTS AND DISCUSSION

Development of the HTS Assays. TR-FRET assays were developed for the binding of SUMO1 to a SUMO1-specific binding peptide referred to as S1 (sequence DNEIECIIVW-EKK) below.[8c] The S1 peptide has more than 10-fold higher affinity for SUMO1 than other tested SIMs for binding either SUMO1 or SUMO2 or 3, and thus enabled the detection of SUMO1-S1 interaction at low concentrations. For GST-tagged SUMO1 and S1 peptide, several detection approaches were tested, including Amplified Luminisecense Proximity Homogenous Assay (ALPHA) Screen, TR-FRET, and FP. The TR-FRET-based assay platform showed the best assay-response window. For the TR-FRET assay, initial steps in assay development involved titration of low-nanomolar concentrations of GST-SUMO1 and Cisbio Tb-anti-GST (Tb) with the fluorescein-tagged S1 peptide. Fluorescein is attached to either the N-terminus (referred to as F-S1) or the C-terminus (referred to as S1F). F-S1 provides better signal-to-background ratio (S/B) than S1F, and it gives near-maximal S/B values at 500 nM (Figure 1A and 1B). Of note, a decrease in the S/B value above 1000 nM, known as a "hook effect", is a result from capping in the specific TR-FRET signal corresponding to SUMO1-S1 binding and concurrent proportional growth of the background (Figure 1C). F-S1 exhibited a smaller assay-response window but greater binding affinity (Figure 1B and 1C). Concentrations of SUMO1 and Tb were further optimized to maximize S/B value using the F-S1 peptide (Figure 1D). Effective displacement of F-S1 by unlabeled S1 confirmed that the fluorescein tag did not significantly alter the binding mode of the S1 peptide and the TR-FRET signal was derived from the desired protein−protein interaction (Figure 1E). DMSO study showed ≤10% signal decline from 1−4% DMSO but no signal change for ≤0.5% DMSO. The data scatter was also reduced by lowering DMSO concentrations, leading to an improved Z' factor and excellent S/B value (Figure 1F, 1G, and 1H). Therefore, this assay is suitable for high-throughput screening (HTS).

An FP assay was developed in parallel with the FRET assay that can serve as a secondary assay using an "orthogonal" detection technology to eliminate false-positive hits in HTS. For this assay, initial assay development involved titration of small amounts of the F-S1 or S1F peptide with GST-SUMO1. Similar to TR-FRET assay results, F-S1 offered a smaller assay-response window but much better binding affinity, with EC_{50} near 1 μM (Figure 1I), consistent with the reported affinity of the SUMO-SIM interaction.[8c] S1F may have a better assay-response window but the binding affinity was lower, which may reflect interference of fluorescein on the interaction, and restricted assay sensitivity to higher compound concentrations. Despite the narrow assay-response window of the F-S1 peptide, the standard deviation among quadruplicates was very low and 2 μM SUMO1 appears sufficient to generate a good Z'-factor in this assay.

Primary HTS. Using the TR-FRET-based biochemical assay (Figure 2A) using GST-labeled SUMO1 PPI and FITC-labeled FS-1 peptide was used to screen the entire MLSMR of ~365 000 compounds at 20 μM in a 1536-well format (PubChem Summary AID 602467). The assay performed robustly with a Z' average over 274 plates of 0.88 and a signal-to background of 4.0. As shown in Figure 2B, the binned data shown in blue as % inhibition shows a Gaussian distribution centered over the negative control shown in pink (wells receiving SUMO1 protein, peptide, and antibody). The positive control is shown in red (well receiving peptide and antibody only). A scatterplot (Figure 2C) of % inhibition vs plate ID showed no well position-specific effects that would have otherwise suggested evaporation or dispenser-related artifacts. After data normalization, 1206 compounds (0.33% hit rate) were selected as initial hits (≥40%I). One known advantage of the TR-FRET assay is its inherent ability to separate real hits from optical artifacts through simple data analysis. Compounds

DOI: 10.1021/co500181b
ACS Comb. Sci. 2015, 17, 239−246

that either absorb at 337 or 490 nm, or fluoresce at 490−520 nm and appear as initial positives judged by TR-FRET signal, are easily detected though their fluorescent intensity in the reference (490 nm) channel. Using the F-ratio parameter (defined as the ratio of fluorescence in a compound well normalized to an average value of fluorescence observed in control wells), we were able to identify hits that have no optical interference issues. Furthermore, we applied additional cheminformatic filtering to eliminate known pan assay interference compounds (PAINS) and promiscuous compounds (PubChem and internal).

Hit Identification. Hits were reconfirmed (36%) in the primary assay. Of these, 176 had potencies (IC_{50}) better than 10 μM, while 24 also had better than 10 μM IC_{50} in the orthogonal FP assay. The final validated hits were analyzed by nuclear magnetic resonance (NMR) spectroscopy to detect the interaction of these compounds with SUMO1. Control experiments using SUMO1 titrated with deuterated DMSO were first acquired to identify solvent effect[12] on NMR chemical shifts. Compounds were titrated to SUMO1 at 0.5:1, 1:1, and 2:1 of compound:SUMO1 stoichiometry to a sample containing 20 μM SUMO1. Similar titration experiments were also conducted for SUMO2 to determine the specificity of these compounds.

We identified a compound with specificity for binding to SUMO1 (Pubmed SID 152137659, CID 3598), which will be referred as SIMI-4 in subsequent discussions (Table 1). It causes significant line-broadening effects on SUMO1 (Figure 3A). The line broadening effects on the SUMO1 resonances suggest that the compound causes chemical shift perturbation (CSP) and that the exchange rate between the free and complex states is in the intermediate regime relative to NMR chemical shift time scale. The residues of SUMO1 that showed line-broadening effects are 22, 35, 37, 43, and 46 upon binding to SIMI-4. These residues are colored in red in Figure 3B. The residues that showed CSP larger than 0.03 ppm (twice the average CSP) upon binding the compound are 38, 42, and 45. These residues are colored in pink in Figure 3B. The chemical shift of a nucleus is sensitive to the changes of its local environment due to a complex formation. Any small additional conformation changes near the direct contacting surfaces will cause additional chemical shift perturbation. Thus, the surface mapped by chemical shift perturbation contains but usually extends beyond the direct binding surface. The data indicate that the compound binds to the surface of SUMO1 that is required for binding SIM, but near one end of the surface including part of the loop connecting the β-strand and α-helix.

This compound does not bind to SUMO2, as indicated by the lack of line broadening effects on SUMO2 upon titration to the SUMO2 sample (Figure 3C). Although CSP was observed on a few residues on the surface opposite from the SIM-binding surface, these residues showed similar CSP when titrating with other analogs, indicating nonspecific effects (Supplementary Figure 1, Supporting Information). The amino acid sequences between SUMO1 and SUMO2 or SUMO3 are nearly identical within the SIM-binding surface, but a significant difference is in the loop connecting the α-helix and β-sheet, which contains a Pro in SUMO2 or 3, but is a His (residue 43, Figure 3B) in SUMO1.[8c] Pro may restrict or alter the conformation of the SIM-binding surface due to the restricted backbone dihedral angles. We tested whether substitution of His-43 of SUMO1 by a Pro affects the compound binding. H43P mutant of SUMO1 is properly folded as shown by the similar chemical shifts as the wild type protein (Figure 3D). However, it no longer binds to the compound, as indicated by the lack of CSP at compound to protein ratio of approximately 4:1, which is twice of that (2:1) when CSP was observed with the wild type SUMO1 (Figure 3A). This result further indicates that the compound binds to the SIM-binding surface of SUMO1 near or including the loop connecting the α-helix and β-strand.

Table 1. Summary of the SUMO-Binding Activities of the SIMI-4 Analogs Estimated by ITC (SIMI-4 and 4-1) and NMR (Other Compounds)

Compound ID	Structure	SUMO1 K_d	SUMO2 K_d
SIMI-4	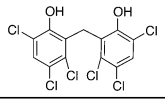	107.60±12.86 μM	> 1 mM
4-1	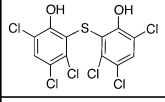	222.72±39.83 μM	> 1 mM
4-2	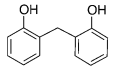	> 1mM	> 1 mM
4-3	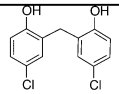	> 1mM	> 1 mM
4-4	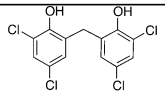	> 1mM	> 1 mM
4-5	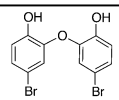	> 1mM	> 1 mM
4-6	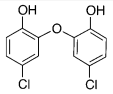	> 1mM	> 1 mM

Purchase and Synthesis of SIMI-4 Analogs. A handful of SIMI-4 compound analogues was purchased or synthesized to explore the SAR for this chemotype. The compounds 4-1, 4-2, 4-3, and 4-4 (Table 1) were purchased from commercial suppliers, and, after analysis for identity and purity, were used as purchased or purified as necessary. The compounds 4-5 and 4-6 (Table 1) were prepared by halogenation of commercially available 2,2′-oxidiphenol as shown in Scheme 1 (and Supporting Information).

Structure−Activity Relationship. Analogs of this compound were tested for binding SUMO1 by NMR studies. Replacement of the carbon atom in the linker by the sulfur atom (4-1) did not significantly change the ability to bind SUMO1, as shown by similar line-broadening effects and CSP in NMR spectra (Supplementary Figure 1, Supporting Information). Removal of the two meta-chlorine atoms (meta- compared to the phenol group) greatly lowered binding affinity, as indicated by the loss of CSP and line-broadening effects (compounds 4-2 to 4-6) (Supplementary Figure 2, Supporting Information). This is unlikely due to electronic effects, because different Cl and Br substitutions on the benzene rings did not lead to recovery of the activity, nor did

DOI: 10.1021/co500181b
ACS Comb. Sci. 2015, 17, 239−246

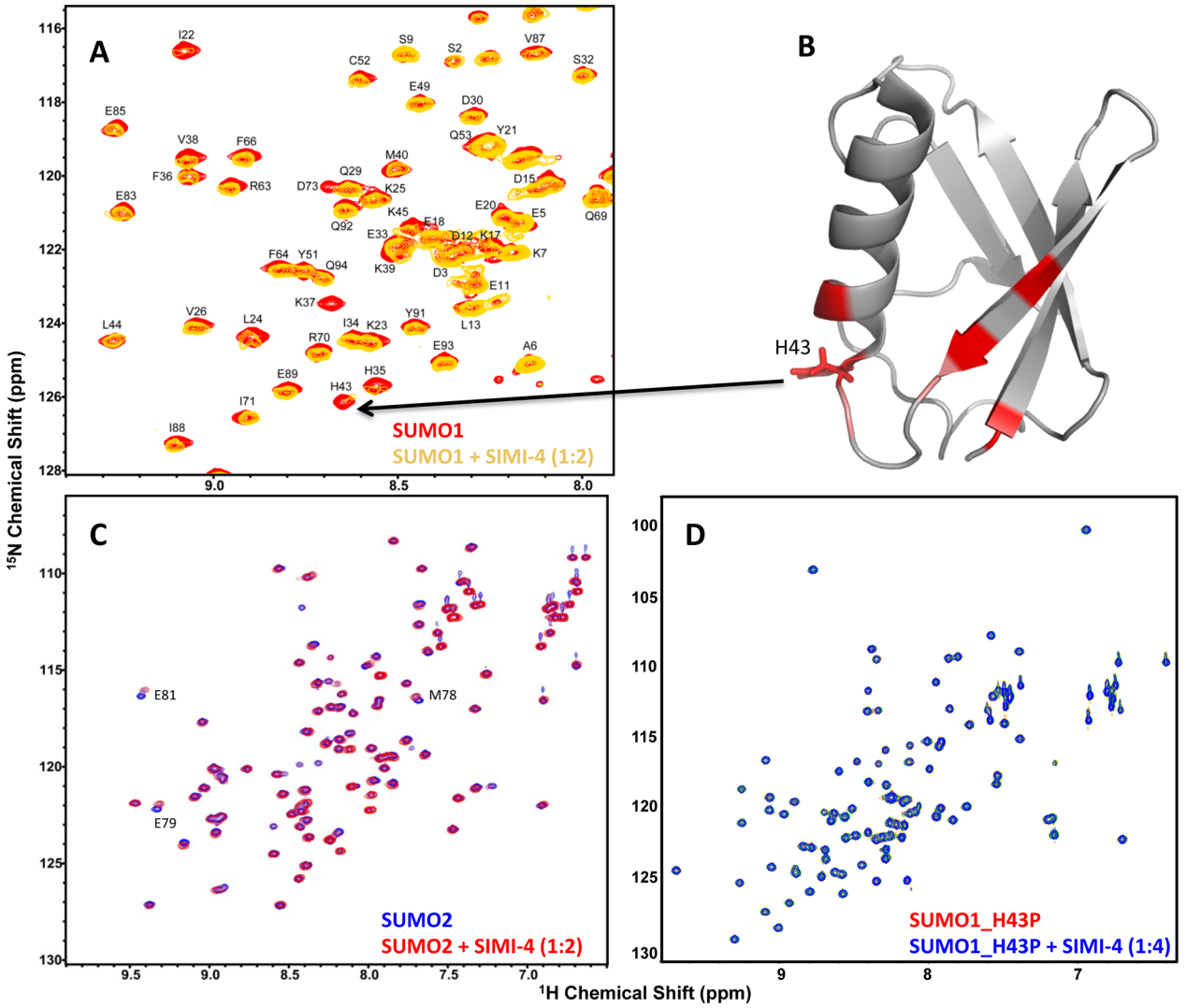

Figure 3. SIMI-4 specifically binds to SUMO1 and not to SUMO2. (A) Expanded view of a region of the superimposed $^{1}H-^{15}N$ HSQC spectra of SUMO1, free (red) and in complex with SIMI-4 (yellow). The assignments of the cross peaks are indicated with their amino acid residue type and number. (B) The structure of SUMO1 with residues that showed severe line-broadening effects indicated in red and significant CSP shown in pink. Residue H43, which showed severe line-broadening effect, is indicated with its side chain. (C) Overlay of the $^{1}H-^{15}N$ HSQC spectra of SUMO2, free (blue) and in complex with SIMI-4 at SUMO:SIMI-4 of 1:2 stoichiometry (red). (D) Overlay of the $^{1}H-^{15}N$ HSQC spectra of SUMO1_H43P mutant, free (red) and in complex with SIMI-4 at different SUMO:SIMI-4 stoichiometry, 1:0.5 (orange), 1:1 (yellow), 1:2 (green), and 4:1 (blue).

Scheme 1. Synthesis of SIMI-4 Analogs[a]

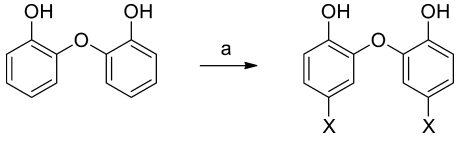

[a]Reagents and conditions: (a) NBS or NCS, PTSA, CH_3CN, rt, 3 h, 58% or 38%, respectively

the replacement of the linker C atom with an O atom (compounds 4-5 and 4-6). The structure–activity relationship suggests that the steric effect provided by the two meta-chlorines is important for the recognition with SUMO1.

The binding affinity of SIMI-4 and 4-1 to SUMO1 was characterized by isothermal titration calorimetry (ITC), which was used to estimate the K_d of 107 ± 13 μM (Figure 4A). K_d was also estimated from NMR chemical shift perturbation and line-shape analysis to be 84 ± 40 μM.[13] Consistent with NMR CSP, the 4-1 analog also binds SUMO with a similar, but slightly lower affinity according to ITC measurements (Supplementary Figure 3, Supporting Information). The interaction is enthalpy driven, with ΔH of −12.8 ± 1.0 kcal/mol for SIMI-4. Similarly, the interaction of the 4-1 analog with SUMO1 is also enthalpy driven, with ΔH of −23.4 ± 3.3 kcal/mol and a larger entropy cost (−60 cal/mol/deg) than SIMI-4 (−24 cal/mol/deg) (Supplementary Figure 3, Supporting Information). The larger entropy cost could reflect the higher flexibility of the thioether linkage than the alkyl linkage. Because NMR can detect interactions with K_d up to 1 mM, the absence of CSP of the other analogs of SIMI-4 indicates that their binding affinities to SUMO1 or SUMO2 have K_d greater than 1 mM.

The affinity of these compounds was not sufficient to inhibit SUMO-SIM interactions required for the E3-ligase activity of RanBP2 (data not shown). Development of protein–protein interaction inhibitors is challenging due to the large surface of the interactions that needs to be blocked by a small molecule.

DOI: 10.1021/co500181b
ACS Comb. Sci. 2015, 17, 239–246

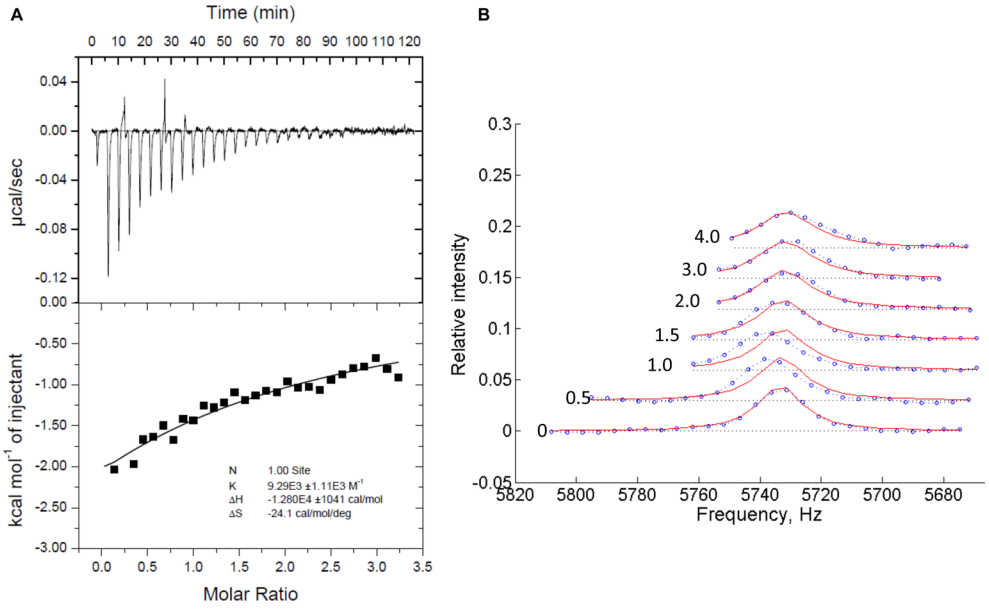

Figure 4. Measurement of the binding affinity between SUMO1 and SIMI-4. (A) Isothermal titration calorimetry (ITC) measurements of compound−SUMO1 interaction. SUMO1 (300 μM in 10 μL increment) was injected to a total volume of 290 μL into a sample cell containing 1.4 mL of 20 μM SIMI-4. Same concentrations of DMSO were added to both the compound and protein solutions in both the experiments. The heat of dilution was subtracted for baseline correction and analyzed with Microcal ORIGIN 5.0 software to extract binding thermodynamic parameters. (B) The 1D slices were extracted with LineShapeKin SPARKY extension from the proton dimension in ^{1}H−^{15}N HSQC spectra (dotted lines) at the SIMI-4:SUMO1 molar ratios of 0, 0.5, 1, 1.5, 2, 3, 4. K_d values were obtained from fitting line shape changes to the Bloch−McConnel equation for a 2-site exchange model using LineShapeKin[13] (solid lines).

Further studies are needed to determine whether modifications of this chemotype to limit the flexibility of the molecule or to increase its size would significantly improve the binding affinity to SUMO1.

Small-molecule inhibitors with specificity to SUMO1 could have therapeutic potential. In a previous study,[8c] we found that expression of S1 peptide in the MCF-7 breast cancer cells was toxic to the cells, but expression of a SUMO2-specific SIM peptide was not, because the SUMO2-specific SIM peptide could be stably expressed in MCF-7 cells, but stable cell lines expressing the S1 peptide could not be established. This suggests that SUMO1 interaction with its SIM is critical for the MCF-7 breast cancer cells.

In summary, the studies show the effectiveness of a multidisciplinary approach to tackle the challenging problem of developing PPI modulators. Further development of such molecules will help to determine the affinities needed to achieve a cellular effect and produce a useful tool to dissect the roles of different SUMO paralogs in regulating cellular functions and validate the specific SUMO paralogs as novel innovative therapeutic targets.

EXPERIMENTAL PROCEDURES

HTS Assays. The initial primary TR-FRET assay was developed and conducted on 363 827 unique compounds in a 1536-well format and is described in PubChem AID 602429. Briefly, 10 nM GST-SUMO1 and 2 nM Tb-anti-GST in 50 mM HEPES pH 7.5, 0.005% Tween 20, and 1 mM DTT were preincubated at room temperature with 20 μM compounds for an hour, followed by addition of 500 nM FITC-labeled S1 peptide (F-S1). Following an additional hour of incubation, the plates were read on a Pherastar (BMG LabTech) with Lanthascreen optical module (ex337/em520, with emission at 490 nm as an internal reference) or with an Envision (PerkinElmer) using their TR-FRET protocol (em340 and ex520/485). Full inhibition controls contained no SUMO1. The assay was robust over the entire screen of 274 plates with a Z' of 0.88.

NMR Studies. Uniformly ^{15}N-labeled mature SUMO1 was expressed and purified as described previously.[14] All ^{15}N-SUMO1 samples (20 μM) used in the NMR screening experiments were in phosphate buffer (20 mM, 1 mM DTT, 90% H_2O, 10% D_2O, pH 6.8). For inhibitor screening, ^{15}N-SUMO1 samples were added with 0.5, 1.0, and 2.0 mol equivalence of the compounds identified from the high throughput screen and transferred to the 96-well SampleJet tubes 5.0 mm (5.0 × 103.5 mm). ^{1}H−^{15}N-HSQC spectra of the samples were collected on Bruker Avance III spectrometer equipped with a cryoprobe operating at 700.243 MHz ^{1}H frequency using the Bruker SampleJet automated sample changer. The weighted proton and nitrogen chemical shifts were calculated and quantified. The final concentrations of deuterated DMSO in all the samples after addition of the compounds were below 2% (v/v). All experiments were carried out at 298 K. NMR data were processed using NMRPipe and analyzed with the program Sparky.[15]

Line shape analysis was carried out by using the software package LineShapeKin.[13] The 1D slices from the proton dimension in ^{1}H−^{15}N HSQC spectra were obtained at the SIMI-4:SUMO1 molar ratios of 0, 0.5, 1, 1.5, 2, 3, 4 from extraction using LineShapeKin SPARKY extension. K_d values were obtained from fitting line shape changes to the Bloch−McConnel equation for a 2-site exchange model.

Isothermal Titration Calorimetry (ITC) Measurements. Microcal (Amherst, MA) VP-ITC calorimeter was used to perform ITC measurements for the binding interaction of SUMO1 with different compounds at 30 °C. SUMO1 and compounds were dissolved in the same buffer (20 mM

DOI: 10.1021/co500181b
ACS Comb. Sci. 2015, 17, 239−246

phosphate buffer, pH 6.8). SUMO1 (300 μM in 10 μL increment) was injected at intervals of 180 s up to a total volume of 290 μL into a sample cell containing 1.4 mL of 20 μM inhibitor. The heat of dilution was measured after each experiment by performing buffer injections into compound using the same experimental concentrations and volumes. In addition, injection of SUMO1 to buffer and to an inactive compound (4−2) was also measured for heat of dilution and control. Same concentrations of DMSO were used in both experiments. The heat of dilution was subtracted for baseline correction and analyzed with Microcal ORIGIN 5.0 software to extract binding thermodynamic parameters.

Chemistry General Procedures. All solvents and reagents were used as received from commercial suppliers, unless noted otherwise. ^{1}H and ^{13}C NMR spectra were recorded on a Bruker AM 400 spectrometer (operating at 400 and 101 MHz respectively) or a Bruker AVIII spectrometer (operating at 500 and 126 MHz, respectively) in $CDCl_3$ with 0.03% TMS as an internal standard. The chemical shifts (δ) reported are given in parts per million (ppm) and the coupling constants (J) are in Hertz (Hz). The spin multiplicities are reported as s = singlet, d = doublet, t = triplet, q = quartet, dd = doublet of doublet, ddd = doublet of doublet of doublet, dt = doublet of triplet, td = triplet of doublet, and m = multiplet. Column chromatography separations were performed using the Teledyne Isco Combi-Flash R_f using RediSep R_f silica gel columns. The analytical RPLC method used an Agilent 1200 RRLC system with UV detection (Agilent 1200 DAD SL) and mass detection (Agilent 6224 TOF). The analytical method conditions included a Waters Aquity BEH C_{18} column (2.1 × 50 mm, 1.7 μm) and elution with a linear gradient of 5% acetonitrile in pH 9.8 buffered aqueous ammonium formate to 100% acetonitrile at 0.4 mL/min flow rate. Automated preparative RP HPLC purification was performed using an Agilent 1200 Mass-Directed Fractionation system (Prep Pump G1361 with gradient extension, makeup pump G1311A, pH modification pump G1311A, HTS PAL autosampler, UV-DAD detection G1315D, fraction collector G1364B, and Agilent 6120 quadrapole spectrometer G6120A). The preparative chromatography conditions included a Waters X-Bridge C18 column (19 × 150 mm, 5 um, with 19 × 10 mm guard column), elution with a water and acetonitrile gradient, which increases 20% in acetonitrile content over 4 min at a flow rate of 20 mL/min (modified to pH 9.8 through addition of NH_4OH by auxiliary pump), and sample dilution in DMSO. The preparative gradient, triggering thresholds, and UV wavelength were selected according to the analytical RP HPLC analysis of each crude sample. Compound purity was measured on the basis of peak integration (area under the curve) from UV−vis absorbance at 214 nm, and compound identity was determined on the basis of mass spectral and NMR analyses. All compounds had >95% purity as determined using the HPLC methods described above.

Compounds SIMI-4 (Princeton Biomolecular, Inc.), 4-1 (Princeton Biomolecular, Inc.), 4-2 (Sigma-Aldrich, Inc.), and 4-3 (Sigma-Aldrich, Inc.) were purchased from commercial sources, and, after analysis for identity and purity, were used as purchased. Compound 4-4 was purchased from Sigma-Aldrich, Inc., and was purified by RP HPLC to 100% purity prior to use.

2,2-Oxybis(4-bromophenol) (4-5). To a solution of 2,2-oxidiphenol (75 mg, 0.396 mmol) and PTSA hydrate (80 mg, 0.396 mmol) in acetonitrile (8 mL) was added *N*-bromosuccinimide (141 mg, 0.791 mmol). The resulting mixture was stirred at room temperature for 3 h, whereupon the mixture was quenched by the addition of 10% $Na_2S_2O_3$ (15 mL), and the layers were separated. The organic layer was washed once with 10% $Na_2S_2O_3$ (15 mL) and twice with water (10 mL), dried ($MgSO_4$), filtered, and concentrated. The residue was purified by flash chromatography (0−20% EtOAc/hexanes gradient) to afford 83 mg (58%) of the compound 4−5 as a colorless solid. ^{1}H NMR (400 MHz, $CDCl_3$): δ 7.21 (dd, J = 8.8 and 2.0 Hz, 2H), 6.99 (d, J = 2.0 Hz, 2H), 6.95 (d, J = 8.8 Hz, 2H), 5.60 (br s, 2H). ^{13}C NMR (126 MHz, $CDCl_3$): δ 146.22, 143.55, 128.53, 121.29, 118.12, 112.18. LC-MS: t_R = 3.38 min, purity =96%. HRMS (m/z): calcd for $C_{12}H_9O_3Br_2$ $(M + H)^+$ 358.8913; found 358.8785.

2,2-Oxybis(4-chlorophenol) (4-6). Following the same procedure used to synthesize 4-5, *N*-chlorosuccinimide was used to produce 4-6 (41 mg, 38%) as an off-white solid. ^{1}H NMR (400 MHz, $CDCl_3$): δ 7.06 (dd, J = 8.8 and 2.4 Hz, 2H), 6.99 (d, J = 8.8 Hz, 2H), 6.86 (d, J = 2.4 Hz, 2H), 5.58 (br s, 2H). ^{13}C NMR (126 MHz, $CDCl_3$): δ 145.67, 143.20, 125.56, 125.44, 118.49, 117.60. LC-MS: t_R = 3.30 min, purity =99%. HRMS (m/z): calcd for $C_{12}H_7O_3Cl_2$ $(M - H)^-$ 268.9778; found 268.9819.

■ ASSOCIATED CONTENT

Ⓢ Supporting Information

^{1}H−^{15}N HSQC spectra, isothermal titration calorimetry measurements, ^{1}H NMR spectra, and ^{13}C NMR spectra. This material is available free of charge via the Internet at http://pubs.acs.org.

■ AUTHOR INFORMATION

Corresponding Author

*E-mail: ychen@coh.org. Phone: 626-930-5408.

Author Contributions

The manuscript was written through contributions of all authors.

Notes

The authors declare the following competing financial interest(s): Dr. Yuan Chen holds equity in SUMO Biosciences LLC.

■ ACKNOWLEDGMENTS

The chemistry effort at the University of Kansas Specialized Chemistry Center was supported by a grant from the NIH Molecular Libraries Probe Production Centers Network to Jeffrey Aubé (PI) (U54HG005031). Support for University of Kansas NMR instrumentation was provided by NIH Shared Instrumentation Grant S10RR024664 and NSF Major Research Instrumentation Grant 0320648. The authors thank Patrick Porubsky (University of Kansas) for compound management and Ben Neuenswander (University of Kansas) for compound purification and high-resolution mass determination. The assay development and HTS efforts were supported by the Molecular Libraries grant U54 HG005033 to John C. Reed at Sanford-Burham Medical Research Institute and by grant 1R21NS066498-01, R01GM086717, and R01GM102538 to Yuan Chen.

■ REFERENCES

(1) (a) Kessler, J. D.; Kahle, K. T.; Sun, T.; Meerbrey, K. L.; Schlabach, M. R.; Schmitt, E. M.; Skinner, S. O.; Xu, Q.; Li, M. Z.; Hartman, Z. C.; Rao, M.; Yu, P.; Dominguez-Vidana, R.; Liang, A. C.;

DOI: 10.1021/co500181b
ACS Comb. Sci. 2015, 17, 239−246

Solimini, N. L.; Bernardi, R. J.; Yu, B.; Hsu, T.; Golding, I.; Luo, J.; Osborne, C. K.; Creighton, C. J.; Hilsenbeck, S. G.; Schiff, R.; Shaw, C. A.; Elledge, S. J.; Westbrook, T. F. A SUMOylation-dependent transcriptional subprogram is required for Myc-driven tumorigenesis. *Science* **2012**, *335* (6066), 348−53. (b) Toyoshima, M.; Howie, H. L.; Imakura, M.; Walsh, R. M.; Annis, J. E.; Chang, A. N.; Frazier, J.; Chau, B. N.; Loboda, A.; Linsley, P. S.; Cleary, M. A.; Park, J. R.; Grandori, C. Functional genomics identifies therapeutic targets for MYC-driven cancer. *Proc. Natl. Acad. Sci. U.S.A.* **2012**, *109* (24), 9545−50.

(2) (a) Li, Y. J.; Stark, J. M.; Chen, D. J.; Ann, D. K.; Chen, Y. Role of SUMO:SIM-mediated protein-protein interaction in non-homologous end joining. *Oncogene* **2010**, *29* (24), 3509−18. (b) Galanty, Y.; Belotserkovskaya, R.; Coates, J.; Polo, S.; Miller, K. M.; Jackson, S. P. Mammalian SUMO E3-ligases PIAS1 and PIAS4 promote responses to DNA double-strand breaks. *Nature* **2009**, *462* (7275), 935−9.

(3) (a) Subramaniam, S.; Sixt, K. M.; Barrow, R.; Snyder, S. H. Rhes, A striatal specific protein, mediates mutant-huntingtin cytotoxicity. *Science* **2009**, *324* (5932), 1327−30. (b) Steffan, J. S.; Agrawal, N.; Pallos, J.; Rockabrand, E.; Trotman, L. C.; Slepko, N.; Illes, K.; Lukacsovich, T.; Zhu, Y. Z.; Cattaneo, E.; Pandolfi, P. P.; Thompson, L. M.; Marsh, J. L. SUMO modification of Huntingtin and Huntington's disease pathology. *Science* **2004**, *304* (5667), 100−4.

(4) (a) Wimmer, P.; Schreiner, S.; Dobner, T. Human pathogens and the host cell SUMOylation system. *J. Virol.* **2012**, *86* (2), 642−54. (b) Bekes, M.; Drag, M. Trojan horse strategies used by pathogens to influence the small ubiquitin-like modifier (SUMO) system of host eukaryotic cells. *J. Innate Immun.* **2012**, *4* (2), 159−67.

(5) (a) Song, J.; Durrin, L. K.; Wilkinson, T. A.; Krontiris, T. G.; Chen, Y. Identification of a SUMO-binding motif that recognizes SUMO-modified proteins. *Proc. Natl. Acad. Sci. U.S.A.* **2004**, *101* (40), 14373−8. (b) Song, J.; Zhang, Z.; Hu, W.; Chen, Y. Small ubiquitin-like modifier (SUMO) recognition of a SUMO binding motif: a reversal of the bound orientation. *J. Biol. Chem.* **2005**, *280* (48), 40122−9.

(6) (a) Hay, R. T. Protein modification by SUMO. *Trends Biochem. Sci.* **2001**, *26* (5), 332−333. (b) Muller, S.; Hoege, C.; Pyrowolakis, G.; Jentsch, S. SUMO, ubiquitin's mysterious cousin. *Nat. Rev. Mol. Cell Biol.* **2001**, *2* (3), 202−10.

(7) Saitoh, H.; Hinchey, J. Functional heterogeneity of small ubiquitin-related protein modifiers SUMO-1 versus SUMO-2/3. *J. Biol. Chem.* **2000**, *275* (9), 6252−8.

(8) (a) Ayaydin, F.; Dasso, M. Distinct in vivo dynamics of vertebrate SUMO paralogues. *Mol. Biol. Cell* **2004**, *15* (12), 5208−18. (b) Zhang, X. D.; Goeres, J.; Zhang, H.; Yen, T. J.; Porter, A. C.; Matunis, M. J. SUMO-2/3 modification and binding regulate the association of CENP-E with kinetochores and progression through mitosis. *Mol. Cell* **2008**, *29* (6), 729−41. (c) Namanja, A. T.; Li, Y. J.; Su, Y.; Wong, S.; Lu, J.; Colson, L. T.; Wu, C.; Li, S. S.; Chen, Y. Insights into high affinity small ubiquitin-like modifier (SUMO) recognition by SUMO-interacting motifs (SIMs) revealed by a combination of NMR and peptide array analysis. *J. Biol. Chem.* **2012**, *287* (5), 3231−40.

(9) Citro, S.; Jaffray, E.; Hay, R. T.; Seiser, C.; Chiocca, S. A role for paralog-specific sumoylation in histone deacetylase 1 stability. *J. Mol. Cell Biol.* **2013**, *5* (6), 416−27.

(10) Li, Y. J.; Perkins, A. L.; Su, Y.; Ma, Y.; Colson, L.; Horne, D. A.; Chen, Y. Gold nanoparticles as a platform for creating a multivalent poly-SUMO chain inhibitor that also augments ionizing radiation. *Proc. Natl. Acad. Sci. U.S.A.* **2012**, *109* (11), 4092−7.

(11) Voet, A. R. D.; Ito, A.; Hirohama, M.; Matsuoka, S.; Tochio, N.; Kigawa, T.; Yoshida, M.; Zhang, K. Y. Discovery of small molecule inhibitors targeting the SUMO−SIM interaction using a protein interface consensus approach. *MedChemComm* **2014**, *5*, 783−786.

(12) Byerly, D. W.; Mcelroy, C. A.; Foster, M. P. Mapping the surface of *Escherichia coli* peptide deformylase by NMR with organic solvents. *Protein Sci.* **2002**, *11* (7), 1850−3.

(13) Kovrigin, E. L.; Loria, J. P. Enzyme dynamics along the reaction coordinate: Critical role of a conserved residue. *Biochemistry* **2006**, *45* (8), 2636−47.

(14) Tatham, M. H.; Kim, S.; Yu, B.; Jaffray, E.; Song, J.; Zheng, J.; Rodriguez, M. S.; Hay, R. T.; Chen, Y. Role of an N-terminal site of Ubc9 in SUMO-1, -2, and -3 Binding and Conjugation. *Biochemistry* **2003**, *42* (33), 9959−69.

(15) (a) Delaglio, F.; Grzesiek, S.; Vuister, G. W.; Zhu, G.; Pfeifer, J.; Bax, A. NMRPipe: A multidimensional spectral processing system based on UNIX pipes. *J. Biomol. NMR* **1995**, *6* (3), 277−93. (b) Goddard, T. D.; Kneller, D. G. *SPARKY 3*; University of California: San Francisco.

DOI: 10.1021/co500181b
ACS Comb. Sci. 2015, 17, 239−246